Supporting Information

Development of Photo-ROS Responsive Liposome for the Delivery of Antibacterial Agent by Targeting Bacterial Membrane

Avijit Mondal, Abir Kayal and Mrinmoy De*

Department of Organic Chemistry, Indian Institute of Science, Bangalore 560012, India

Email: md@iisc.ac.in

EXPERIMENTAL SECTION:

1. Materials and methods: All reagents and solvents were purchased from commercial sources (Sigma Aldrich and SRL India Pvt. Ltd.) and were used without further purification. NMR spectra were measured using a Bruker 400 MHz spectrometer with TMS (tetramethylsilane) as an internal standard. The NMR data are reported as δ (ppm), representing the chemical shift value relative to TMS. Peak multiplicities are denoted as follows: s = singlet, d = doublet, t = triplet, q = quartet, br = broad, and m = multiplet. High-resolution mass spectra were recorded on a XEVO G2-XS QTof instrument. AFM images were acquired using a JPK instrument and processed with JPK software. UV-Visible spectra were recorded on a Shimadzu UV-3600 UV-Vis-NIR spectrophotometer. Photoluminescence spectra were recorded on a Thermo Scientific Varioskan Flash Multimode Reader. The zeta potential and hydrodynamic diameter were measured using a Malvern Zetasizer Nano instrument. TEM images of the quantum dots were obtained using a FEI Tecnai T20 Super Twin microscope operating at 200 kV. SEM images of bacteria were recorded using an Ultra55 FE-SEM Karl Zeiss EDS instrument.

2. Ligand synthesis:

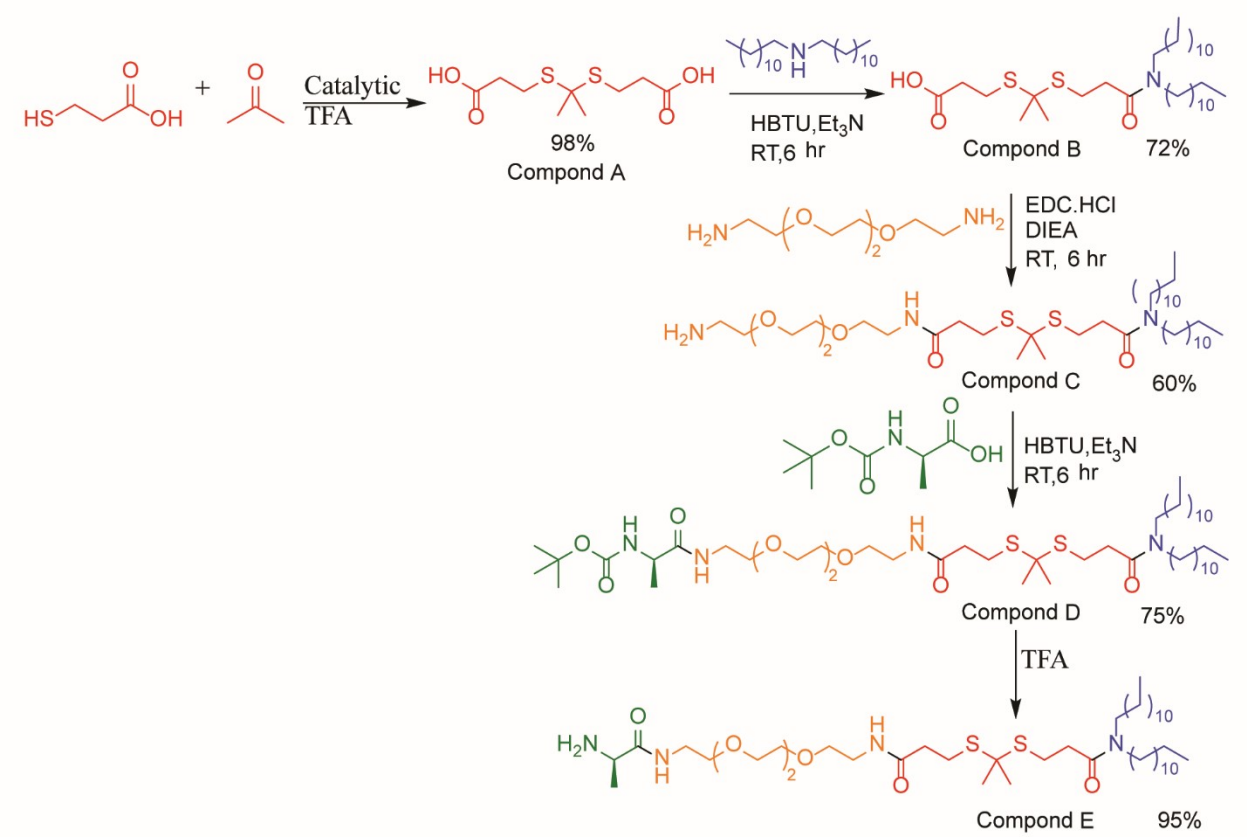

Fig. S1. Scheme of synthesis of lipid molecule.

Compound A : Synthesis of $^1O_2$-cleavable thioketal (TK). 3-mercaptopropionic acid (5 g, 47.2 mmol) was added to acetone (1.3 g, 21.46 mmol) in presence catalytic amount of trifluoroacetic acid (TFA) (20 µL) and the mixture was allowed to stir at room temperature for 8 hr. At the end of the reaction, the white precipitated thus formed was washed with hexane and cold water. The overall yield for the product was 98%. The product was confirmed through ^{1}H NMR and HRMS spectra.

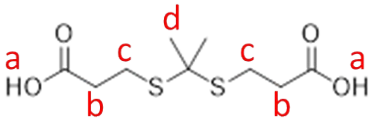

^{1}H NMR (400 MHz, $CDCl_3$, TMS): δ 11.74 (s, 2H, -COO**H** (a)), 2.85 – 2.82 (t, 4H, -S**CH_2**- (c), J = 7.2 Hz), 2.66 – 2.63 (t, 4H, -(b) **CH_2**-COOH, J = 7.6 Hz), 1.57 (s, 6H, -(**CH_3**)$_2$(d)).

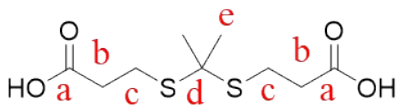

^{13}C NMR (100 MHz, $CDCl_3$, TMS): δ 178.5 (-**C**OOH (a)), 56.4 (-**C**$(CH_3)_2$S-)(d), 34.0 (-**C**H_2COOH (b)), 30.7 (-C(**C**$H_3)_2$S-) (e), 24.7 (-S**C**H_2CH_2-) (c).

MS (ESI+): m/z Calculated for $C_{23}H_{65}NO_3S_2N$ $([M+Na])^+$ (charge= +1): 275.0388, Found 275.0388

Compound B. Compound A (0.48 mmol, 1.0 equiv.) was dissolved in dry dichloromethane (10 mL) within a round bottom flask fitted with a magnetic stir bar and positioned on an ice-bath. Subsequently, HBTU (0.58 mmol, 1.2 equiv.) and triethyl amine (1.93 mmol, 4 equiv.) were added to the solution. The resulting mixture was stirred for 15 minutes. Following this, didodecylamine was introduced (0.24 mmol, 0.5 equiv.), and the reaction mixture was allowed to stir at room temperature for 6 hours under an argon atmosphere. Upon completion of the reaction, the resulting mixture underwent washing with water (2x15 mL), and the organic layer was subsequently dried over sodium sulfate. Ater evaporating the solvent, the residue was loaded onto a SiO_2 column for purification, affording compound B. The overall yields typically ranged around 72%. After purification the presence of the compounds were confirmed by ^{1}H NMR and HRMS spectra.

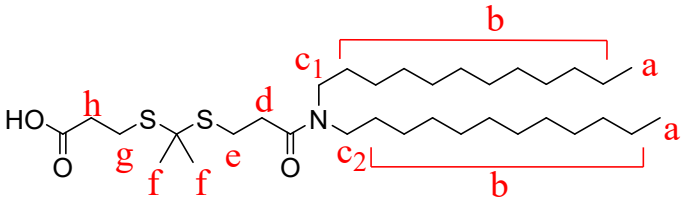

^{1}H NMR (400 MHz, $CDCl_3$, TMS): δ 3.31-3.27 (t, J = 7.6, 2H, -*(*c_1*)***C**H_2-N-CH_2-), δ 3.22-3.18 (t, J = 7.7, 2 H, -CH_2-N-**C**H_2*(*c_2*)*-), δ 2.93-2.87 (m, 4 H, -S-C**H**$_2$-(g,e)), δ 2.67-2.58 (m, 4 H, - CO-C**H**$_2$-(h,d)), δ 1.60 (s, 6H, -(C**H**$_3)_2$)(f), δ 1.54-1.25 (m, 40 H, -C**H**$_2$-(b)), δ 0.89-0.86 (t, J = 6.6 Hz, 6 H, -C**H**$_3$)(a).

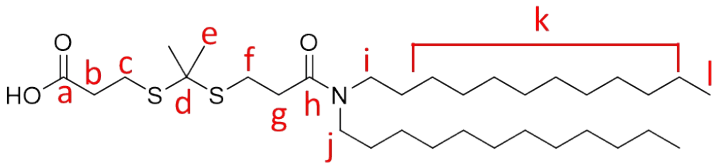

^{13}C NMR (100 MHz, $CDCl_3$, TMS): δ 175.8 (-**C**OOH)(a), 171.1 (-CH_2**C**ON)(h), 56.2 (-**C**$(CH_3)_2$S-)(e), 48.2 (-N**C**H_2-)(i), 46.4 (-N**C**H_2-)(j), 34.5 (-**C**H_2COOH)(b), 32.5 (-S**C**H_2CH_2-)(c), 31.9 (alkyl chain)(k), 30.8(alkyl chain)(k), 29.6(alkyl chain)(k), 29.4(alkyl chain)(k), 29.3(alkyl chain)(k), 29.1(alkyl chain)(k), 27.7 (-**C**H_2CH_2CON-)(f), 27.0 (-CH_2**C**H_2CON-)(g), 25.8(alkyl chain)(k), 25.2(alkyl chain)(k), 22.7 (-C(**C**$H_3)_2$S-)(e), 14.1(-**C**H_3)(l).

MS (ESI$^+$): m/z Calculated for $C_{23}H_{65}NO_3S_2N$ ($[M+Na]^+$ (charge= +1) : 610.4304, Found 610.4302

Compound C. A solution of compound B (0.5 mmol, 1 equiv.) in dichloromethane (DCM) (50 mL) was treated with N,N-Diisopropylethylamine (DIEA) (2 mmol, 4 equiv.). The reaction mixture was subsequently cooled to 0°C and reacted with EDC-HCl (0.6 mmol, 1.2 equiv.). Following a 15-minute stirring period, 2,2'-((oxybis(ethane-2,1-diyl))bis(oxy))bis(ethan-1-amine) (5 mmol, 10 equiv.) was added to the reaction mixture, which was then stirred for 6 hours at room temperature. Upon completion of the reaction, dichloromethane was evaporated, and the resulting product was extracted with hexane (50 mL × 6). The hexane extracts were evaporated, and the crude mixture was subjected to purification by column chromatography. Compound C was obtained with an overall yield of 60%. Post-purification, the presence of the compounds was confirmed through ^{1}H NMR and HRMS spectra analysis.

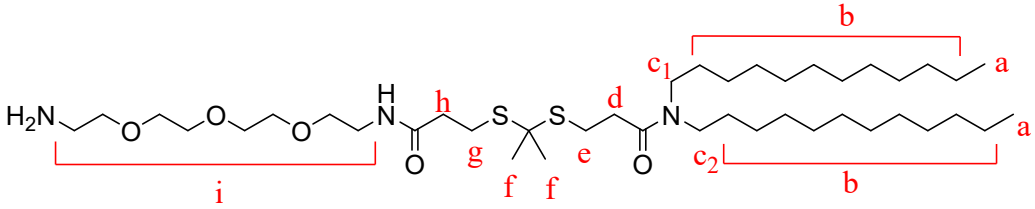

^{1}H NMR (400 MHz, $CDCl_3$, TMS): δ 3.63-3.44 (m, 16 H, -N-C**H**$_2$-C**H**$_2$-O-C**H**$_2$-C**H**$_2$-O-C**H**$_2$-C**H**$_2$-O-C**H**$_2$-C**H**$_2$-N (i)), δ 3.29-3.25 (t, J=7.9 Hz, 2 H, -**C**H_2(*c$_1$*)-N-CH_2-), δ 3.20-3.16 (t, J= 7.6 Hz, 2 H, -CH_2-N-**C**H_2(*c$_2$*)-), δ 2.91-2.86 (m, 4 H, - S-C**H**$_2$-(g,e)), δ 2.58-2.55 (t, J= 7.4 Hz, 2 H, -

CO-C**H**$_2$-(h), δ 2.48-2.45 (t, J= 7.3 Hz, 2 H, - CO-C**H**$_2$-(d)), δ 1.59 (s, 6H, -(C**H**$_3$)$_2$)(f), δ 1.52-1.24 (m, 40 H, -C**H**$_2$-(b)), δ 0.88-0.85 (t, J=6.4 Hz, 6 H, -C**H**$_3$)(a).

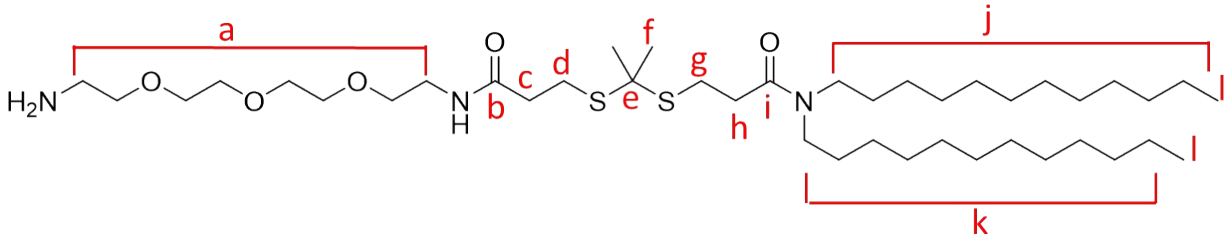

^{13}C NMR (100 MHz, CDCl$_3$, TMS): δ 171.4 (-NH**C**O-(b)), 170.5 (-**C**ON-(i)), 82.9 (NH$_2$**C**H$_2$-(a)), 73.1(NH$_2$CH$_2$**C**H$_2$-)(a),71.0(NH$_2$CH$_2$CH$_2$O**C**H$_2$-)(a),70.4(NH$_2$CH$_2$CH$_2$OCH$_2$**C**H$_2$-)(a),70.4 (NH$_2$CH$_2$CH$_2$OCH$_2$CH$_2$O**C**H$_2$-)(a),70.0(NH$_2$CH$_2$CH$_2$OCH$_2$CH$_2$OCH$_2$**C**H$_2$-)(a),69.8(NH$_2$CH$_2$CH$_2$OCH$_2$CH$_2$OCH$_2$CH$_2$O**C**H$_2$-)(a), 55.8 (NH$_2$CH$_2$CH$_2$OCH$_2$CH$_2$OCH$_2$CH$_2$OCH$_2$**C**H$_2$-)(a), 54.3(-**C**(CH$_3$)$_2$S-)(e), 50.4 (-N**C**H$_2$-)(j), 48.0 (-N**C**H$_2$-(k)), 46.2(-NHCO**C**H$_2$-)(c), 45.3 (-NHCOCH$_2$**C**H$_2$S-)(d), 41.3 (-S**C**H$_2$CH$_2$CON-)(g), 39.1(-SCH$_2$**C**H$_2$CON-)(h), 38.5 (alkyl chain)(j or k), 36.1 (alkyl chain)(j or k), 36.0(alkyl chain)(j or k), 36.0 (alkyl chain)(j or k), 32.6 (alkyl chain)(j or k), 32.5 (alkyl chain)(j or k), 31.8 (alkyl chain)(j or k), 31.6 (alkyl chain)(j or k), 30.8 (alkyl chain)(j or k), 29.6 (alkyl chain)(j or k), 29.6 (alkyl chain)(j or k), 29.5 (alkyl chain)(j or k), 29.4 (alkyl chain)(j or k), 29.3 (alkyl chain)(j or k), 29.1 (alkyl chain)(j or k), 27.7 (alkyl chain)(j or k), 27.0 (alkyl chain)(j or k), 26.9 (alkyl chain)(j or k), 26.0 (alkyl chain)(j or k), 25.9 (alkyl chain)(j or k), 25.7 (alkyl chain)(j or k), 22.6 (-C(**C**H$_3$)$_2$S-)(f), 14.1 (-**C**H$_3$)(l).

MS (ESI$^+$): m/z Calculated for $C_{41}H_{83}N_3O_5S_2$ $([M+H])^+$ (charge= +1): 762.5852, Found 762.5850

Compound D. The synthetic procedure for compound D closely resembles that of compound B. Nonetheless, in this reaction, compound C and a protected amino acid were utilized in a 1:1 equivalent ratio. The resulting product underwent purification via column chromatography, yielding an overall compound yield of 75%. Following purification, the presence of the compounds was validated through analysis of ^{1}H NMR and HRMS spectra.

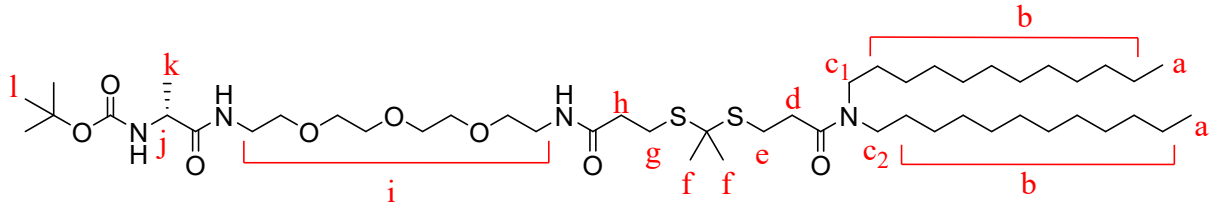

[1]H NMR (400 MHz, CD_3OD , TMS): δ 4.08 (br, 1 H, -NH-C**H**-CO-)(j), δ 3.66-3.55 (m, 16 H-N-C**H**$_2$-C**H**$_2$-O-C**H**$_2$-C**H**$_2$-O-C**H**$_2$-C**H**$_2$-O-C**H**$_2$-C**H**$_2$-N-(i)), δ 3.40-3.37 (m, 4 H, -C**H**$_2$-N-C**H**$_2$-)(c_1 and c_2), δ 2.91-2.87 (m, 4 H, -S-C**H**$_2$-(g,e)), δ 2.69-2.66 (t, J= 7.2 Hz, 2 H, - CO-C**H**$_2$-(h)), δ 2.52-2.48 (m, 2 H, - CO-C**H**$_2$-(d)), δ 1.60 (s, 6H, -(C**H**$_3$)$_2$)(f), δ 1.46 (s, 9H, -C(C**H**$_3$)$_3$)(l), δ 1.31 (br, 43H, - CH-**CH**$_3$, -CH_2-)(b), δ 0.93-0.90 (t, J=6.7 Hz, 6 H, -CH_3)(a).

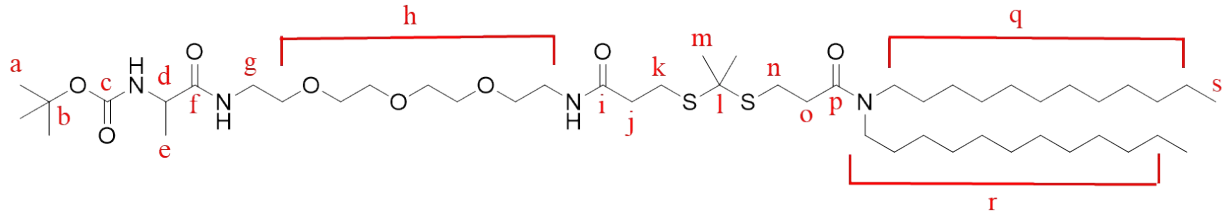

[13]C NMR (100 MHz, CD_3OD, TMS): δ 172.6 (-CH(CH_3)**C**O**N**H-)(f), 171.7 (-NH**C**OCH_2-)(i), 170.3 (-O**C**O**N**H-)(c), 156.1 (CH_2**C**O**N**-)(p), 79.1(-NH**C**$\mathbf{H_2}$-)(g), 70.2(-NHCH$_2$**C**$\mathbf{H_2}$-)(h), 69.8(-NHCH$_2$CH$_2$O**C**$\mathbf{H_2}$-)(h), 69.2(-NHCH$_2$CH$_2$OCH$_2$**C**$\mathbf{H_2}$-)(h), 69.1(-NHCH$_2$CH$_2$OCH$_2$CH$_2$O**C**$\mathbf{H_2}$-)(h), 62.8(-NHCH$_2$CH$_2$OCH$_2$CH$_2$OCH$_2$**C**$\mathbf{H_2}$-)(h), 62.7(-NHCH$_2$CH$_2$OCH$_2$CH$_2$OCH$_2$CH$_2$O**C**$\mathbf{H_2}$-)(h), 55.5(-NHCH$_2$CH$_2$OCH$_2$CH$_2$OCH$_2$CH$_2$OCH$_2$**C**$\mathbf{H_2}$-)(h), 50.2(-**C**(CH_3)$_2$S-)(l), 46.0 (-N**C**$\mathbf{H_2}$-)(q,r), 42.2 (-N**C**$\mathbf{H_2}$-)(q,r), 42.0(-NHCO**C**$\mathbf{H_2}$-)(j), 39.1(-NHCOCH$_2$**C**$\mathbf{H_2}$S-)(k), 39.0(-S**C**$\mathbf{H_2}$CH$_2$CON-)(n), 38.9(-SCH$_2$**C**$\mathbf{H_2}$CON-)(o), 37.5(alkyl chain)(q,r), 36.0(alkyl chain)(q,r), 35.4(alkyl chain)(q,r), 33.2(alkyl chain)(q,r), 32.7(alkyl chain)(q,r), 31.7(alkyl chain)(q,r), 30.0(alkyl chain)(q,r), 29.4(alkyl chain)(q,r), 29.4(alkyl chain)(q,r), 29.3(alkyl chain)(q,r), 29.2(alkyl chain)(q,r), 29.1(alkyl chain)(q,r), 29.0(alkyl chain)(q,r), 28.7(alkyl chain)(q,r), 28.5(alkyl chain)(q,r), 27.3(alkyl chain)(q,r), 26.6(alkyl chain)(q,r), 26.5(alkyl chain)(q,r), 26.4(alkyl chain)(q,r), 25.7(alkyl chain)(q,r), 25.6(alkyl chain)(q,r), 24.5(alkyl chain)(q,r), 22.3(alkyl chain)(q,r), 19.5(alkyl chain)(q,r), 19.4(alkyl chain)(q,r), 17.3(-C(**C**$\mathbf{H_3}$)$_2$S-)(m), 13.1(-**C**$\mathbf{H_3}$)(s).

MS (ESI$^+$): m/z Calculated for $C_{49}H_{96}N_4O_8S_2$ ([M+Na])$^+$ (charge= +1): 955.6567, Found 955.6569

Compound E. Compound D (0.5 mmol, 1 equiv.) was dissolved in dichloromethane (DCM), to which Trifluoroacetic Acid (TFA) (1 mL) was added. The reaction mixture was stirred for 3 hours, after which the solvents were removed under vacuum. The resulting product was obtained with an overall yield of 95%. Characterization of the compound was conducted through ^{1}H NMR and HRMS spectroscopy.

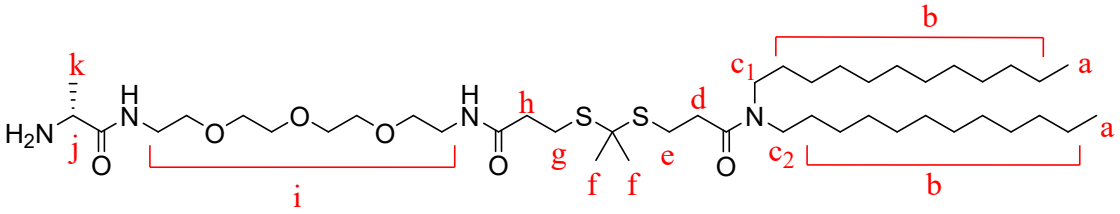

^{1}H NMR (400 MHz, CD_3OD, TMS): δ 3.70-3.54 (m, 16 H, N-C**H$_2$**-C**H$_2$**-O-C**H$_2$**-C**H$_2$**-O-C**H$_2$**-C**H$_2$**-O-C**H$_2$**-C**H$_2$**-N-(i)), δ 3.40-3.36 (m, 4 H, -C**H$_2$**-N-C**H$_2$**-(c_1 and c_2), δ 3.26-3.20 (q, J= 7.3 Hz, J= 7.3 Hz, 1 H, -NH-C**H**-CO-(j)), δ 3.02 (br, 4 H, -N**H**-, -N**H$_2$**), δ 2.91-2.87 (m, 4 H, -S-C**H$_2$**-(g,e), δ 2.69-2.66 (t, J=7.2 Hz, 2 H, -CO-C**H$_2$**-(h)), δ 2.52-2.48 (t, J=7.2 Hz, 2 H, -CO-C**H$_2$**-(d)), δ 1.60 (s, 6H, -(C**H$_3$**)$_2$)(f), δ 1.31 (br, 43H, - CH-C**H$_3$**,(k) -CH_2-(b)), δ 0.93-0.90 (t, J= 6.7 Hz, 6 H, -C**H$_3$**)(a).

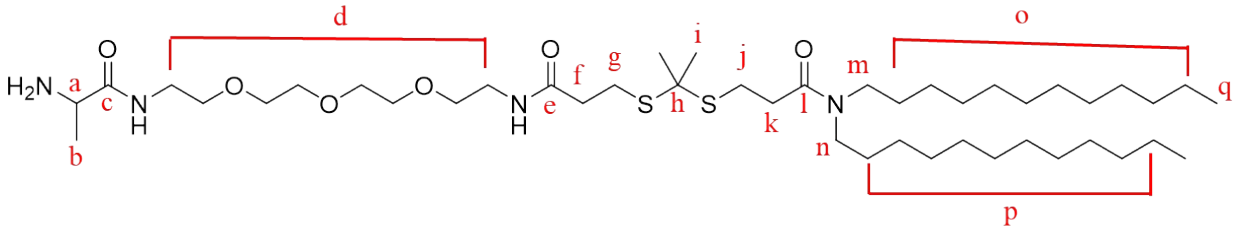

^{13}C NMR (100 MHz, CD_3OD, TMS): δ 172.6(-CH(CH_3)**C**ONH-)(c), 171.7(-NH**C**OCH_2-)(e), 162.6(CH_2**C**ON-)(l), 70.1(-NH**C**H$_2$-)(d), 70.1(-NHCH_2**C**H$_2$-)(d), 69.9(-NHCH_2CH_2O**C**H$_2$-)(d), 69.8(-NH$CH_2CH_2OCH_2$**C**H$_2$-)(d), 69.1(-NH$CH_2CH_2OCH_2CH_2O$**C**H$_2$-)(d),69.1(-NH$CH_2CH_2OCH_2CH_2OCH_2$**C**H$_2$-)(d),55.6(-NH$CH_2CH_2OCH_2CH_2OCH_2CH_2O$**C**H$_2$-)(d), 48.4(-NH$CH_2CH_2OCH_2CH_2OCH_2CH_2OCH_2$**C**H$_2$-)(d), 46.5(-**C**($CH_3$)$_2$S-)(h), 46.0(-N**C**H$_2$-)(m), 44.6(-N**C**H$_2$-)(n), 39.1(-NHCO**C**H$_2$-)(f), 39.0(-NHCO$CH_2$**C**H$_2$S-)(g), 38.9(-S**C**H$_2CH_2$CON-)(j), 38.8(-S$CH_2$**C**H$_2$CON-)(k), 35.4(alkyl chain)(o or p), 32.7(alkyl chain)(o or p), 31.7(alkyl chain)(o or p),

30.8(alkyl chain)(o or p), 29.9(alkyl chain)(o or p), 29.4(alkyl chain)(o or p), 29.3(alkyl chain)(o or p), 29.2(alkyl chain)(o or p), 29.1(alkyl chain)(o or p), 29.0(alkyl chain)(o or p), 28.7(alkyl chain)(o or p), 27.3(alkyl chain)(o or p), 26.6(alkyl chain)(o or p), 26.4(alkyl chain)(o or p), 25.7(alkyl chain)(o or p), 25.6(alkyl chain)(o or p), 22.3(alkyl chain)(o or p), 21.1(-C(**C**$\mathbf{H_3}$)$_2$S-)(i), 13.1(-**C**$\mathbf{H_3}$)(q), 7.8(-CH(**C**$\mathbf{H_3}$)CONH-)(b).

MS (ESI$^+$): m/z calculated for $C_{44}H_{88}N_4O_6S_2$ $[M+H]^+$ (charge = +1): 833.6224; found: 833.6224

3. Liposome formulation and encapsulation

Liposomes were prepared using established methodologies as described previously.[1, 2] The synthesized lipid molecules, including cholesterol, DSPC, and DMG-PEG2000, were dissolved in ethanol. This solution was then mixed at a molar ratio of 50:38.5:10:1.5 in a solvent consisting of 90% ethanol and 10% 10mM sodium citrate (by volume). Rapid pipette mixing facilitated the spontaneous formation of liposomes. Following liposome formation, dialysis (14 kDa MWCO) against PBS for 6 hours was conducted to remove residual ethanol.

For the encapsulation of SQD and Pos-SQD, liposomes were formed in the presence of SQD in ethanol. Subsequently, unencapsulated SQD was eliminated through dialysis (14 kDa MWCO) against PBS (14 kDa MWCO) for a duration of 48 hours. The encapsulation efficiency

$$\text{Encapsulation Efficiency (\%)} = \frac{F_{total} - F_{unencapsulated}}{F_{total}} \times 100$$

is calculated as

For SQD the encapsulation efficiency is 72% and for Pos-SQD the encapsulation efficiency is 63%.

4. Synthesis and functionalization of SQDs

For the synthesis of SQDs, we utilized the bottom-up hydrothermal method established by our research group.[3] In brief, a mixture of sublimed sulfur and p-phenylenediamine in a 1:1 ratio was subjected to hydrothermal heating at 200°C for 24 hours, with tetraethylene glycol serving as a stabilizer. Following completion of the reaction, the crude mixture underwent purification via

column chromatography. Subsequently, the formation of SQDs was confirmed through various characterization techniques.

To impart a positive charge to the surface of SQDs, we synthesized a positively charged thiol ligand according to previously reported literature. The synthesized positively charged ligand is characterized by ^{1}H NMR spectroscopy (Fig. S14). Surface functionalization of SQDs was achieved by adding the thiol ligand and stirring for 48 hours. At the end of the 48-hour period, any unbound ligands were removed via DCM workup. The observed shift in zeta potential from -7.74 mV to +57.5 mV provided confirmation of successful surface functionalization (Fig. S15).

5. Antibacterial activity

The antibacterial effectiveness of Pos-SQD and Pos-SQD@Liposome was evaluated against methicillin-resistant *S. aureus* (MRSA, USA300) bacteria. Initially, freeze-dried bacterial species were revived on nutrient agar plates by incubation at 37°C. The resulting bacterial colonies were then cultured overnight (10-12 hours) in Luria broth media (LB, HiMedia-20 g/L) to prepare the primary culture. Subsequently, a secondary culture was prepared by inoculating 100 µL of the primary culture into 10 mL of fresh LB and incubating at 37°C until it reached the mid-log phase (OD620nm~0.3). The optical density of bacterial suspensions was adjusted to OD_{620nm}=0.01 (equivalent to 10^6 to 10^7 bacteria/mL) for further experimentation. In 96-well plates, 100 µL of bacterial solutions were combined with 100 µL of materials at varying concentrations. The growth of bacteria was monitored over a period of 16 hours using a microplate reader equipped with a shaker and incubator set at 37°C. The minimum concentration of functionalized SQDs at which no increase in growth curves was observed was identified as the Minimum Inhibitory Concentration (MIC).

To assess the stimuli-responsive antibacterial activity of Pos-SQD@Liposome, MRSA bacteria with an OD of 0.01 were first incubated with different concentrations of Pos-SQD@Liposome in the dark for 2 hours to facilitate internalization. Following the 2-hour incubation period, the samples were irradiated with white light (40W LED lamp) to induce destabilization of the liposomes via singlet oxygen generation, consequently releasing the

encapsulated Pos-SQD, which exhibited antibacterial activity. The same experiment is carried out for only Pos-SQD for control study.

6. Live/dead assay using fluorescence microscopy

The antibacterial efficacy of Pos-SQD@Liposome was evaluated by simultaneously staining bacteria with Syto-9 (green) and propidium iodide (red). Initially, MRSA bacteria were harvested via centrifugation at 5000 rpm and resuspended in PBS. The bacterial suspension was then treated with Pos-SQD@Liposome in dark for 2 hours, followed by 1 hour of light irradiation. Post-treatment, the bacterial solution underwent two washes with PBS and was subsequently stained with 4 μM of Syto-9 and propidium iodide for 30 minutes. Excess dye was removed by centrifugation, and the bacterial suspension was resuspended in PBS buffer. Following this, 10 μL of the stained bacterial solution was drop-casted onto a clean glass slide for visualization under a confocal microscope.

7. SEM imaging of MRSA bacteria

For scanning electron microscopy (SEM) sample preparation, MRSA bacteria with an optical density of 0.01 in PBS were incubated with Pos-SQD@Liposome in dark for 2 hours, followed by 1 hour of light irradiation. Following incubation, any unbound materials were removed through centrifugation at 5000 rpm for 5 minutes. The treated bacterial pellets were then suspended in 3% glutaraldehyde in PBS and allowed to incubate for 1 hour. Subsequently, the solution underwent centrifugation to accumulate the cells, which were then dehydrated using various ethanol gradients (30%, 50%, 70%, and 100%). Following dehydration, 10 μL of the solution was drop-casted onto a silicon wafer and subjected to gold sputtering before imaging in SEM.

8. Cell viability assay

The cytotoxicity of Pos-SQD@Liposome was evaluated against *HeLa* cell lines using the MTT assay. Initially, *HeLa* cells were seeded onto a 96-well plate at a density of 15000 cells/mL and allowed to incubate for 24 hours in Dulbecco's Modified Eagle Medium (DMEM). Following this incubation period, varying concentrations of Pos-SQD (for control) and Pos-SQD@Liposome were added to the wells, and the cells were further incubated for 24 hours. After this incubation, cell viability was assessed using the MTT dye, which is converted by viable cells into insoluble

formazan crystals over a 4-hour incubation period. The formazan crystals were then dissolved in DMSO, and the relative cell viability was determined by measuring the absorbance at 570 nm.

Additional Figures

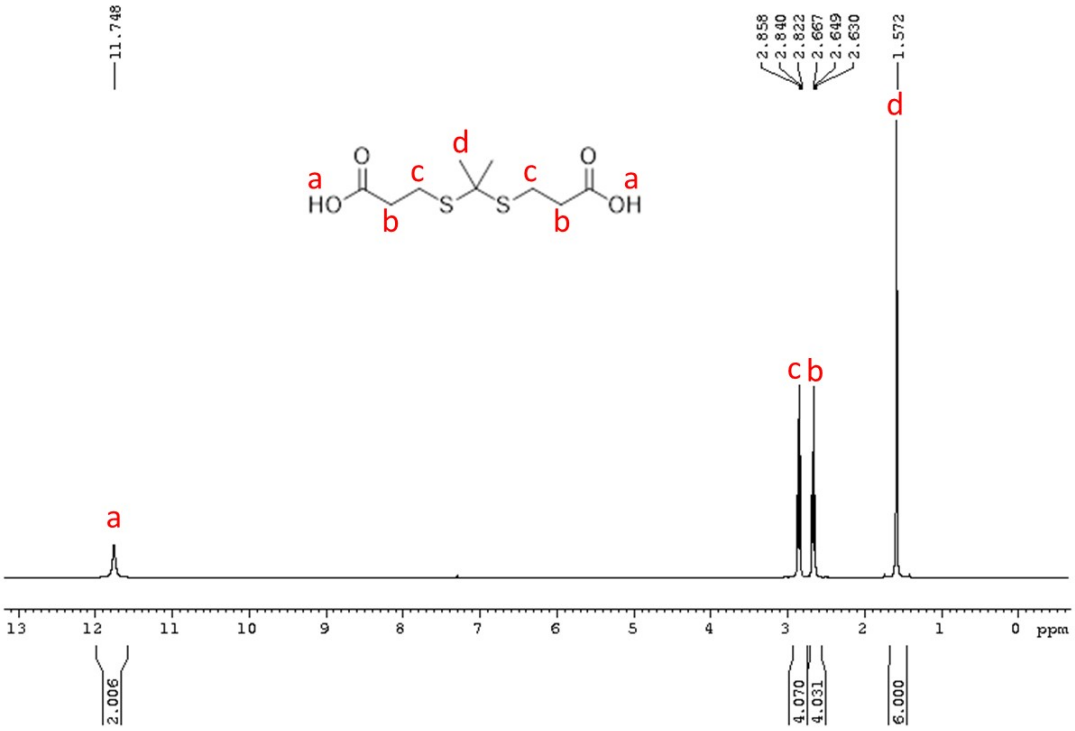

9. ^{1}H NMR spectrum of Compound A

Fig. S2. ^{1}H NMR spectrum of Compound A

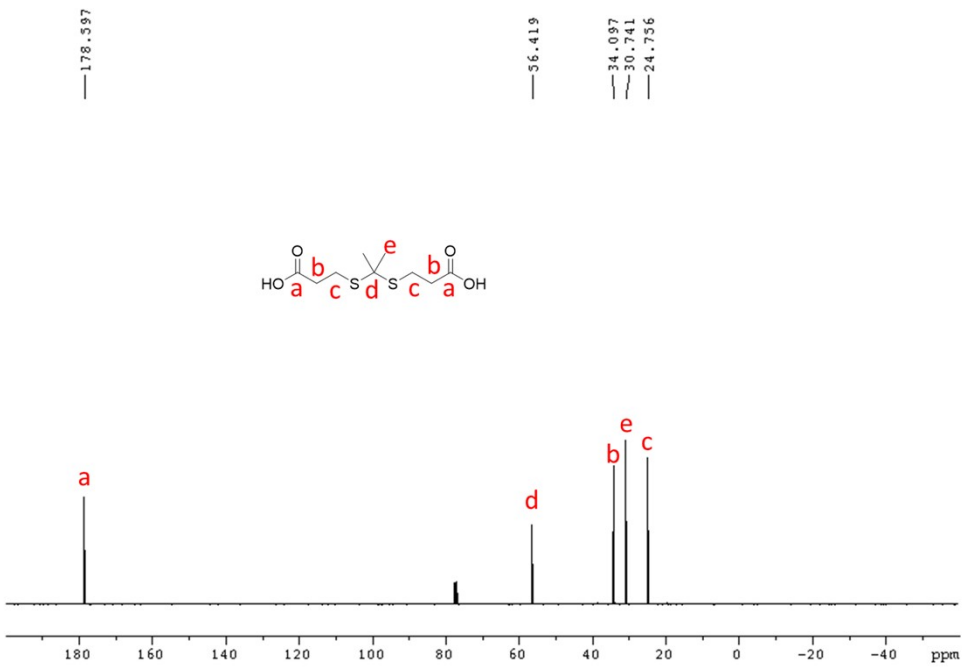

10. ^{13}C NMR spectrum of Compound A

Fig. S3. ^{13}C NMR spectrum of Compound A

11. Mass spectrum of compound A

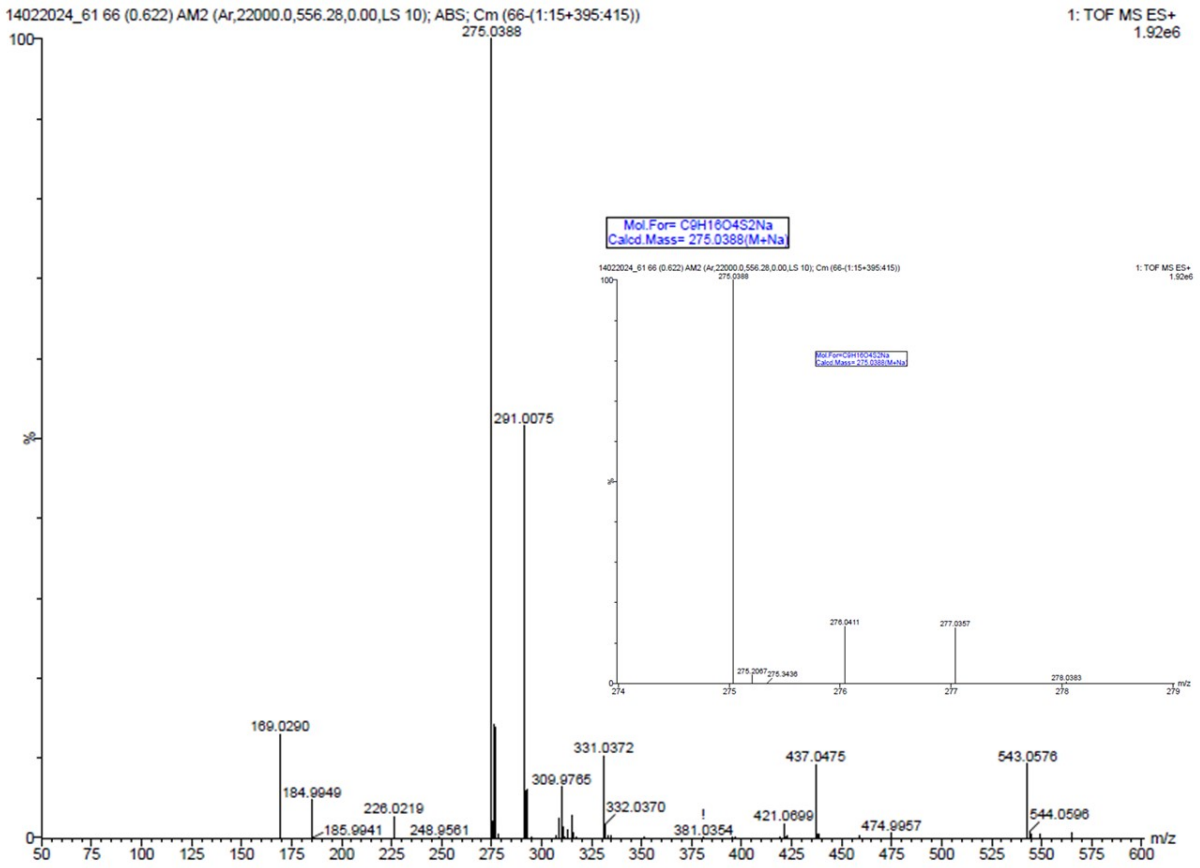

Fig. S4. Mass spectrum of compound A. Inset: magnified view of the molecular ion region.

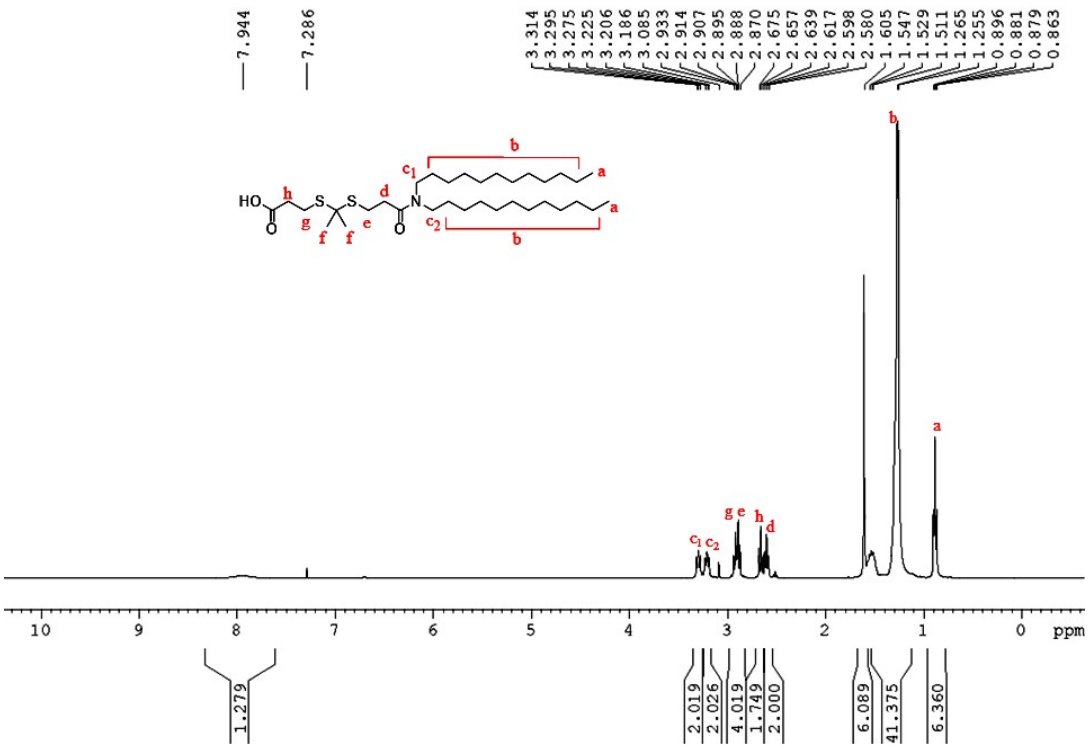

12. ^{1}H NMR spectrum of Compound B

Fig S5. ^{1}H NMR spectrum of Compound B.

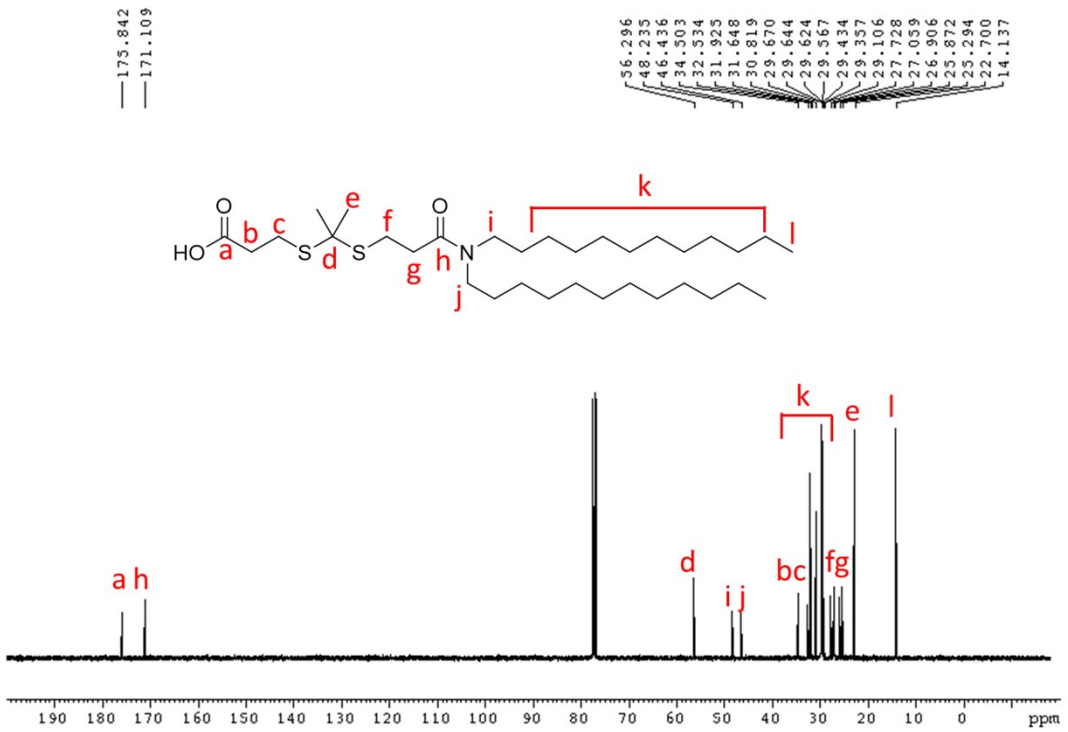

13. ^{13}C NMR spectrum of Compound B

Fig S6. ^{13}C NMR spectrum of Compound B.

14. Mass spectrum of Compound B

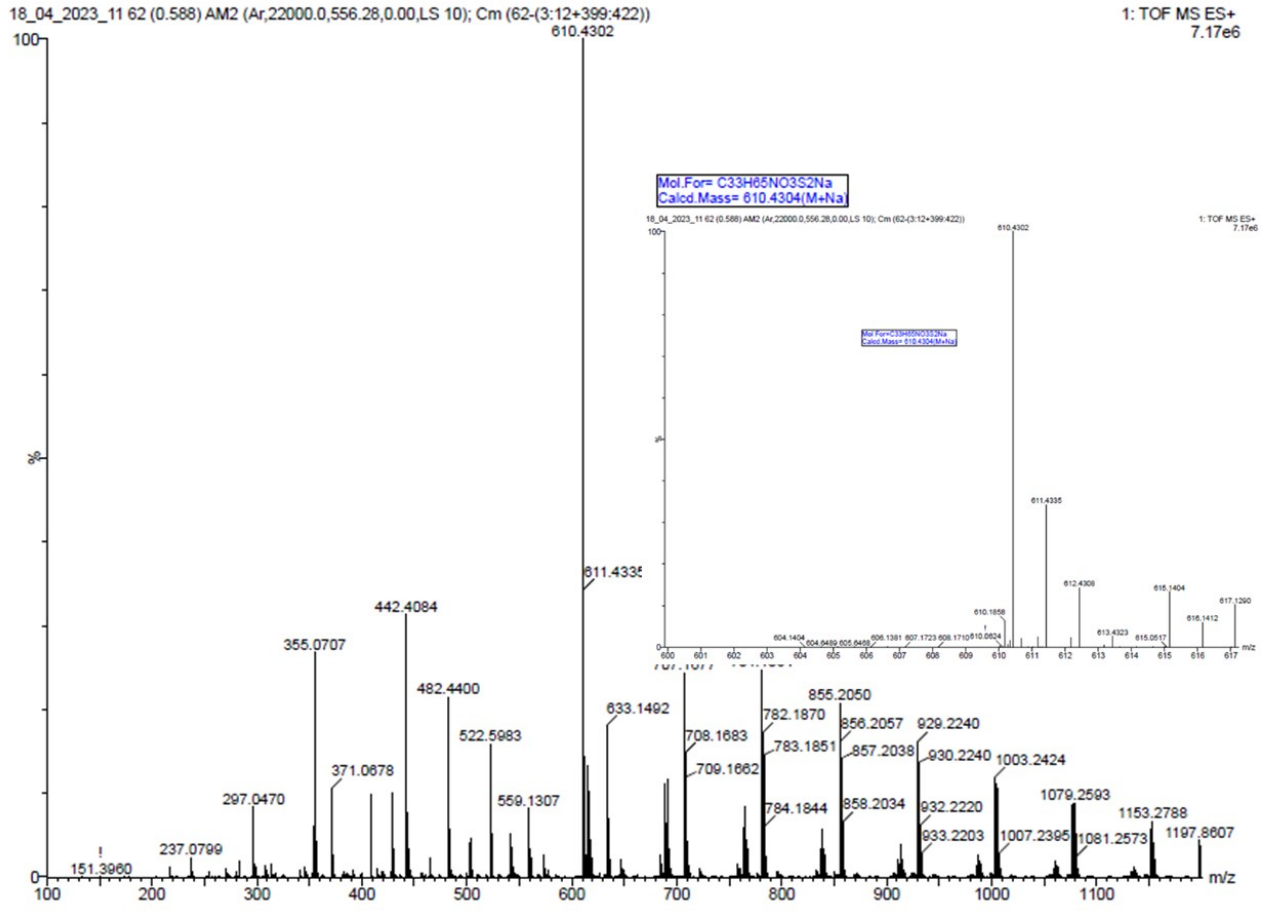

Fig S7. Mass spectrum of Compound B. Inset: magnified view of the molecular ion region.

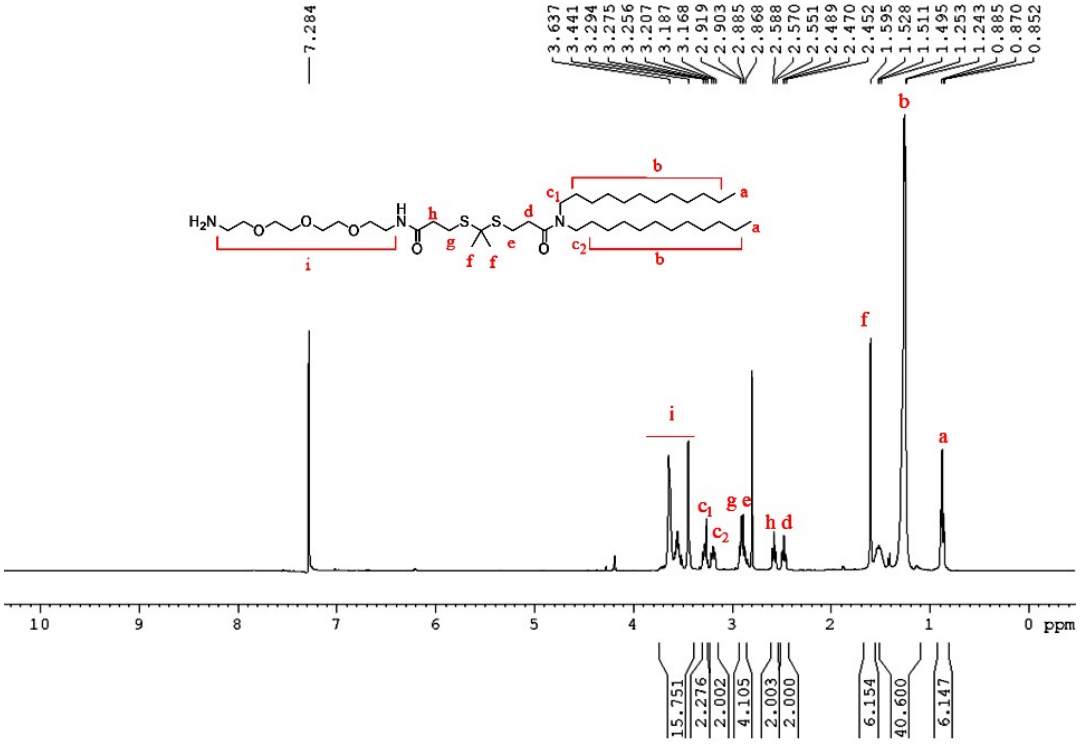

15. ^{1}H NMR spectrum of Compound C

Fig S8. ^{1}H NMR spectrum of Compound C.

16. ^{13}C NMR spectrum of Compound C

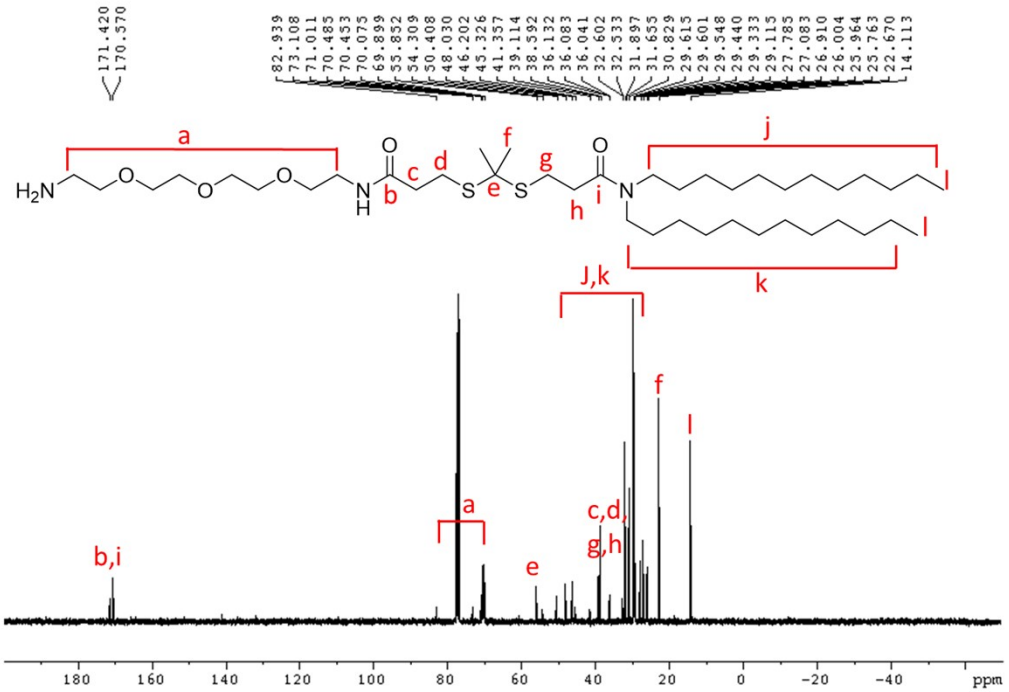

Fig S9. ^{13}C NMR spectrum of Compound C.

17. Mass spectrum of Compound C

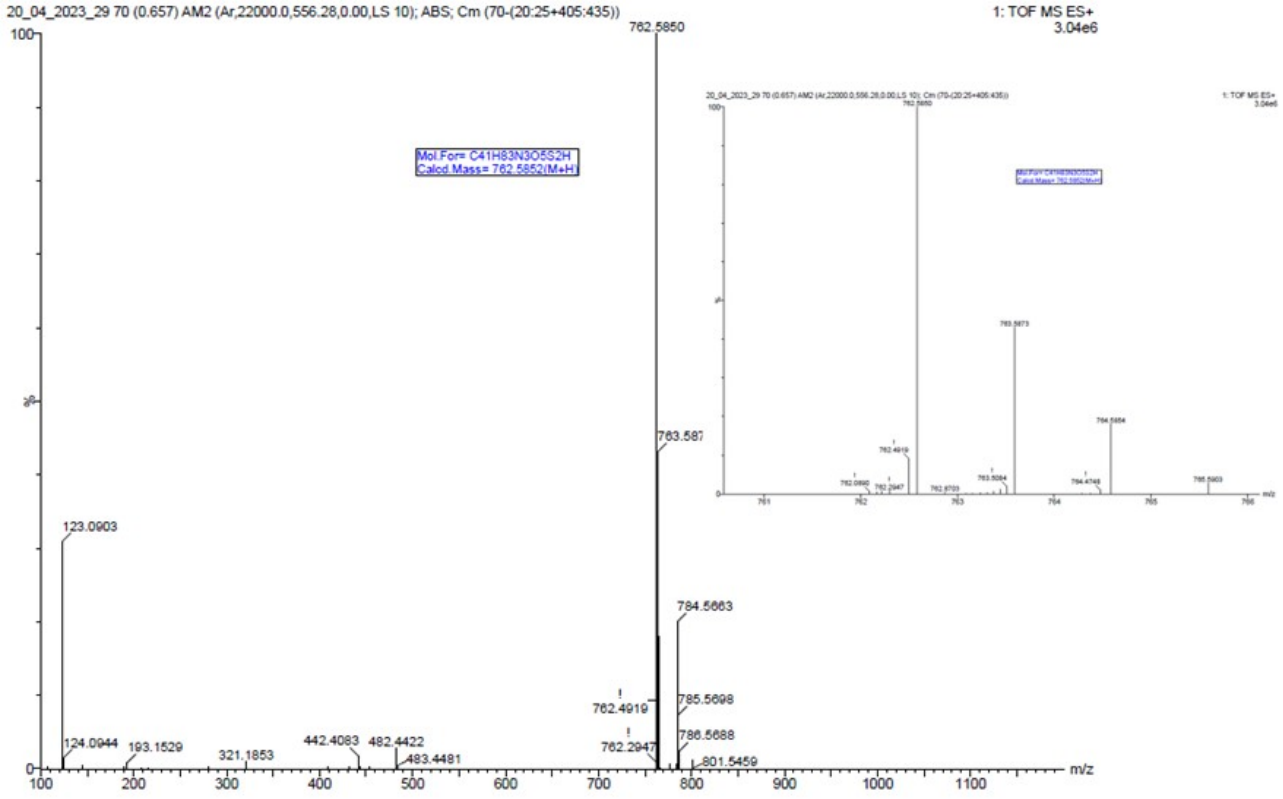

Fig. S10. Mass spectrum of Compound C. Inset: magnified view of the molecular ion region.

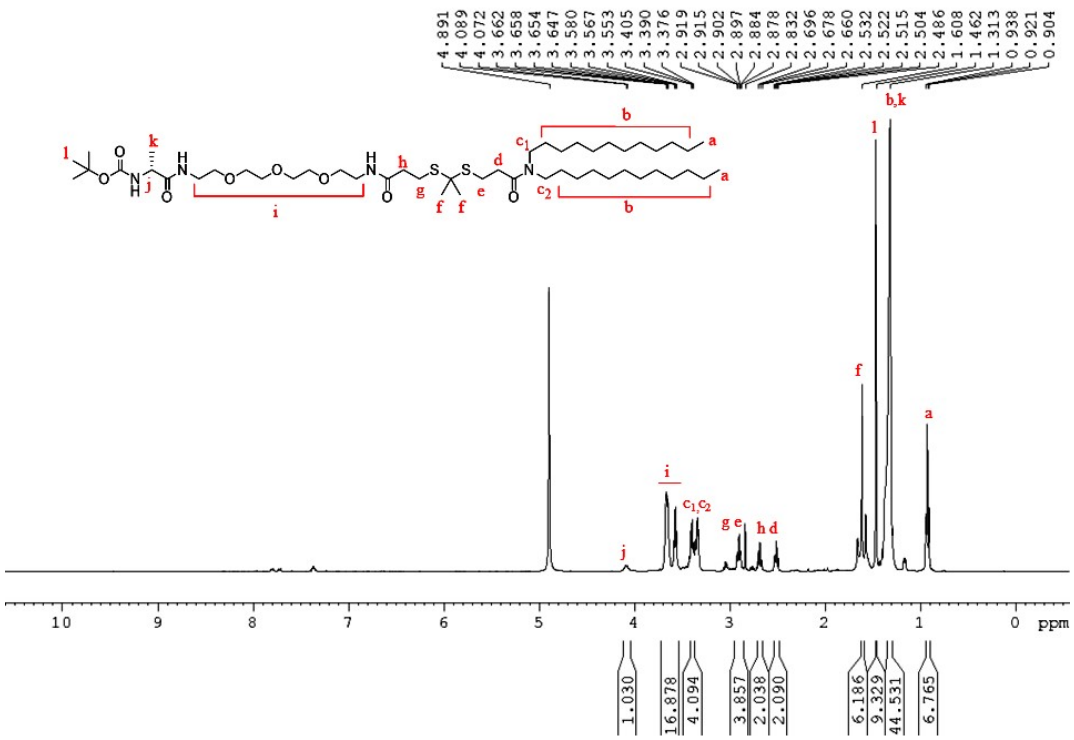

18. ^{1}H NMR spectrum of Compound D

Fig S11. ^{1}H NMR spectrum of Compound D.

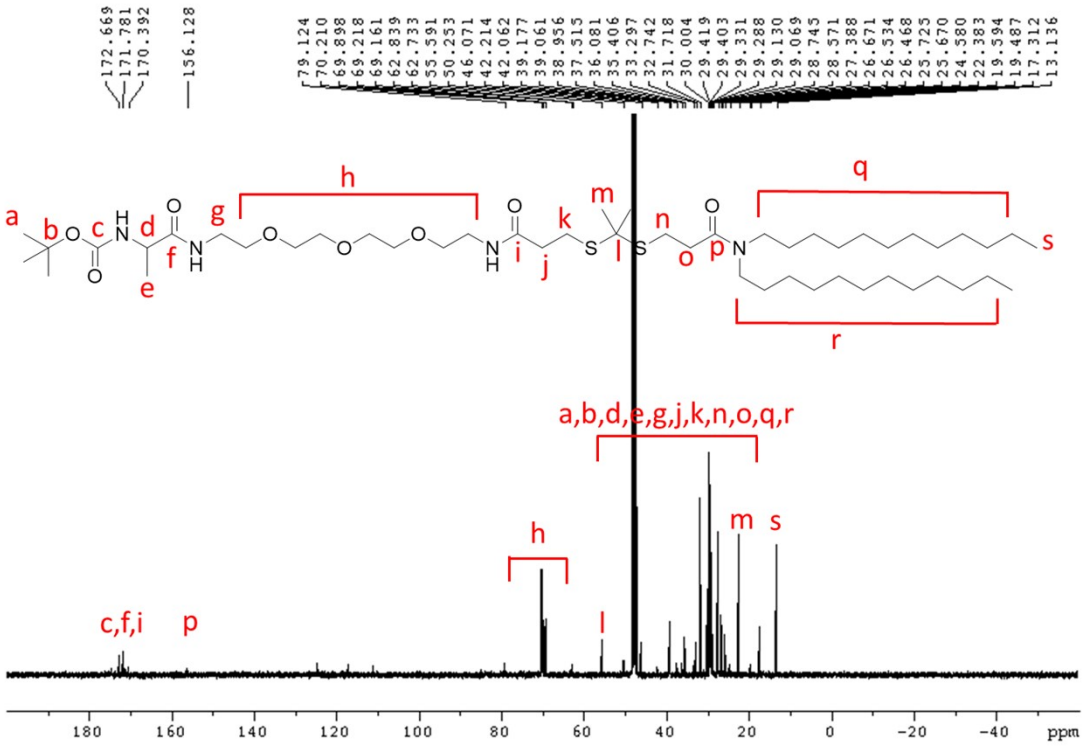

19. ^{13}C NMR spectrum of Compound D

Fig S12. ^{13}C NMR spectrum of Compound D.

20. Mass spectrum of Compound D

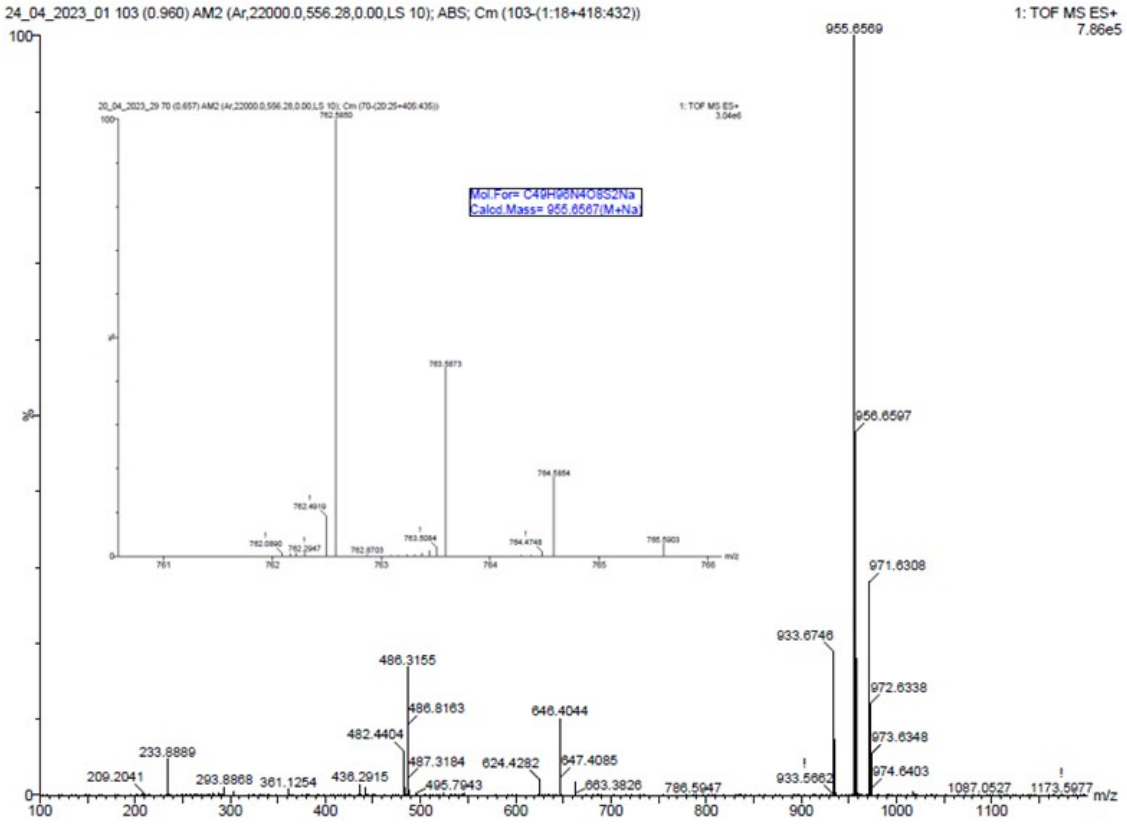

Fig S13. Mass spectrum of Compound D. Inset: magnified view of the molecular ion region.

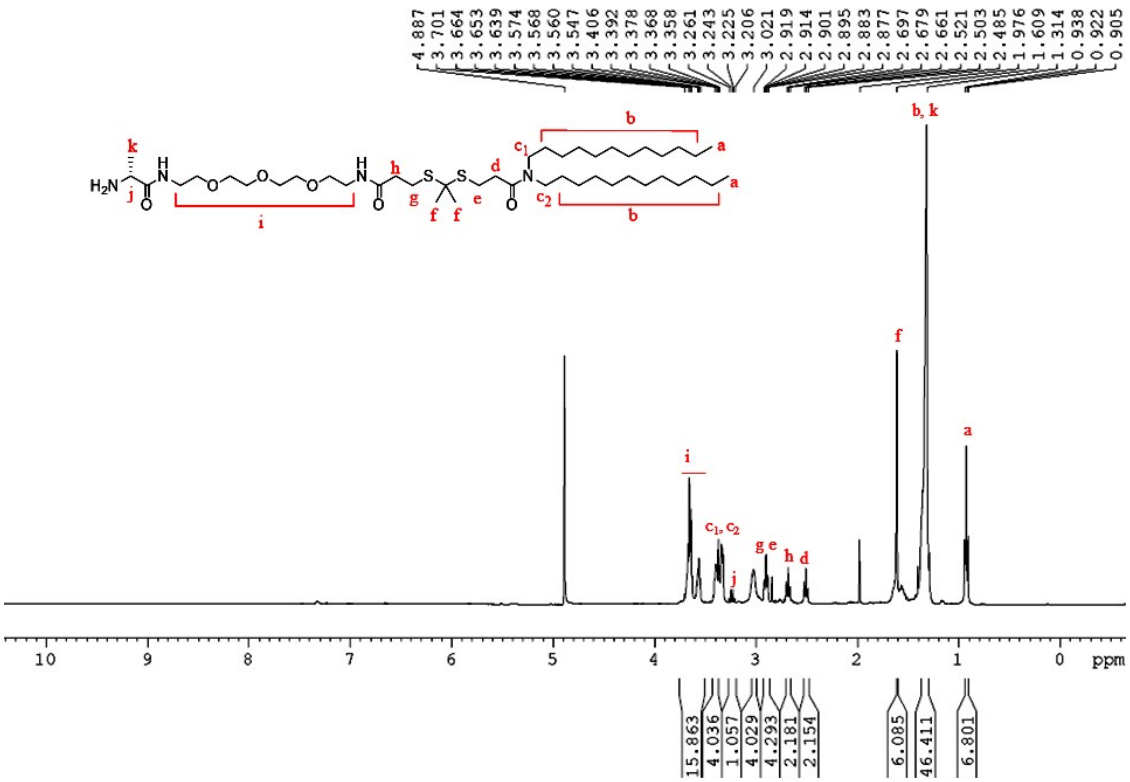

21. ^{1}H NMR spectrum of Compound E

Fig S14. ^{1}H NMR spectrum of Compound E.

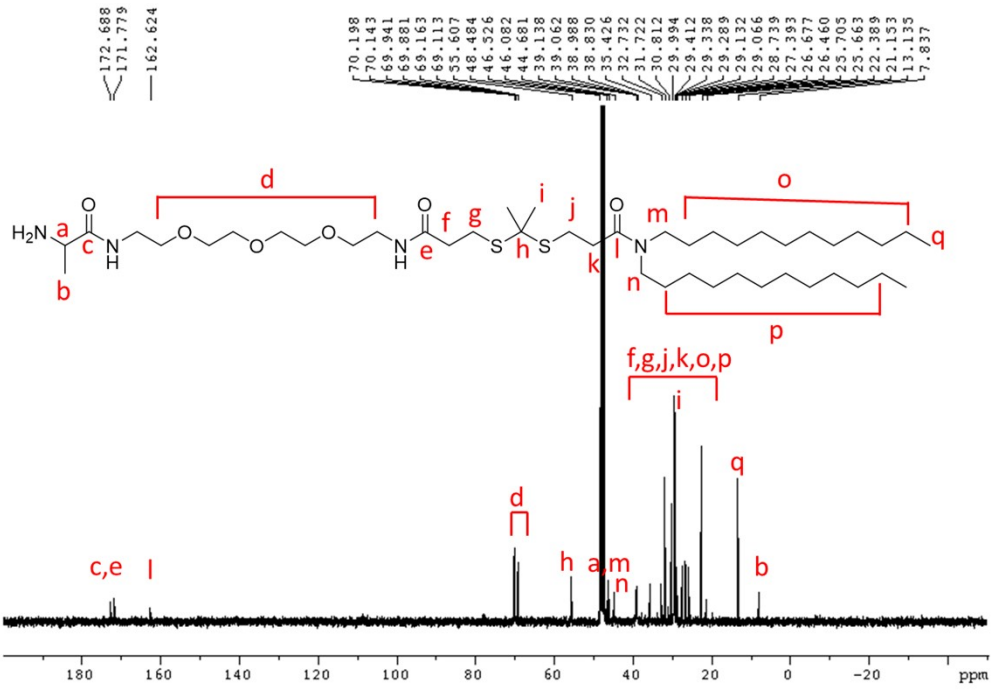

22. ^{13}C NMR spectrum of Compound E

Fig S15. ^{13}C NMR spectrum of Compound E.

23. Two-Dimensional (2D) NMR spectrum of Compound E

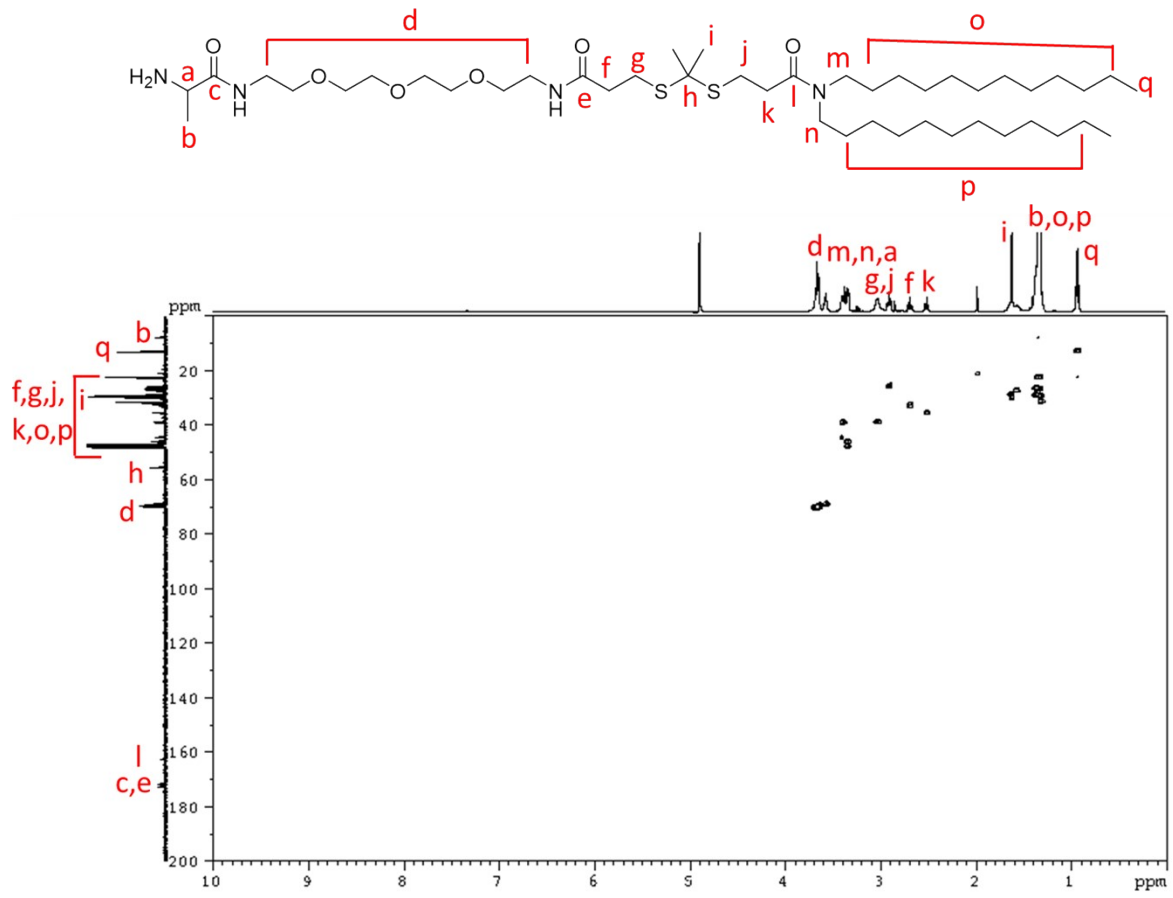

Fig S16. HSQC NMR spectrum of Compound E.

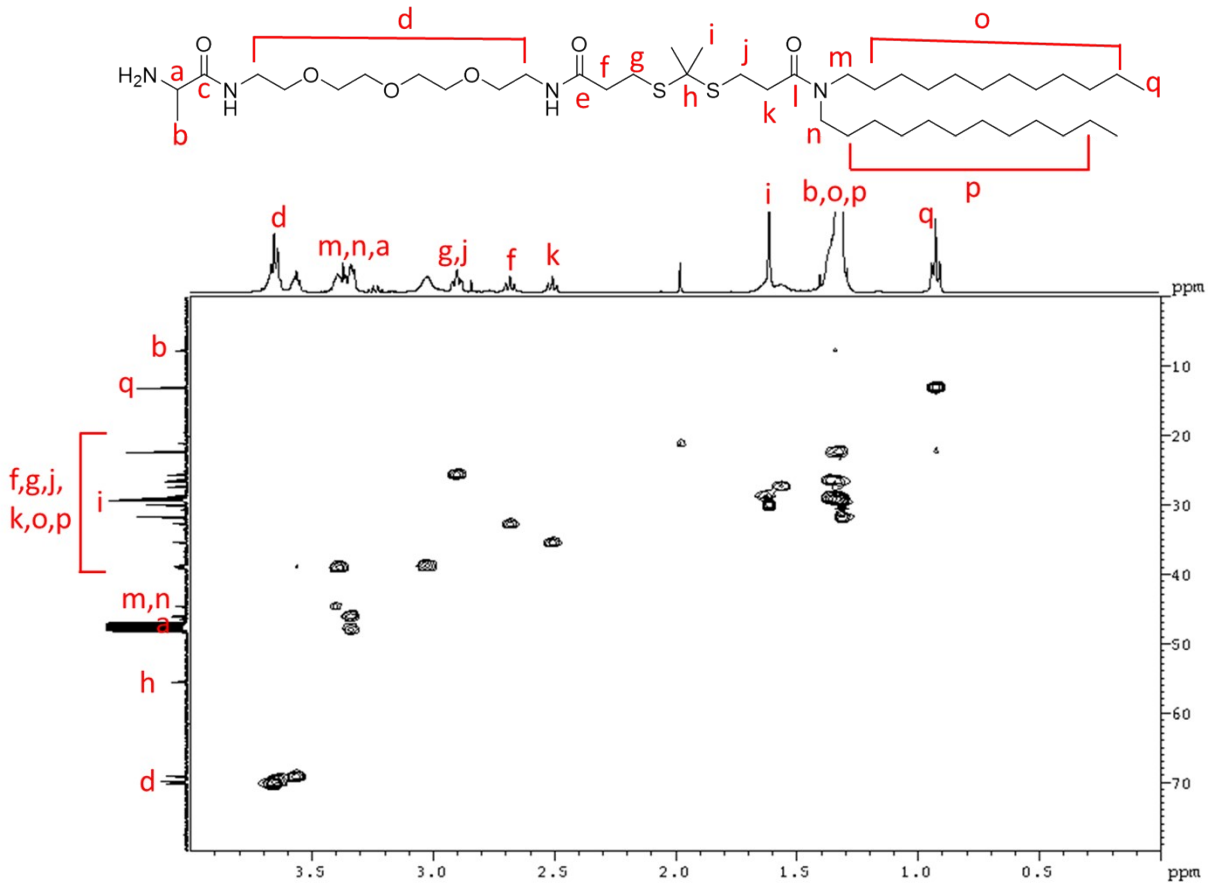

Fig S17. Magnified HSQC NMR spectrum of Compound E.

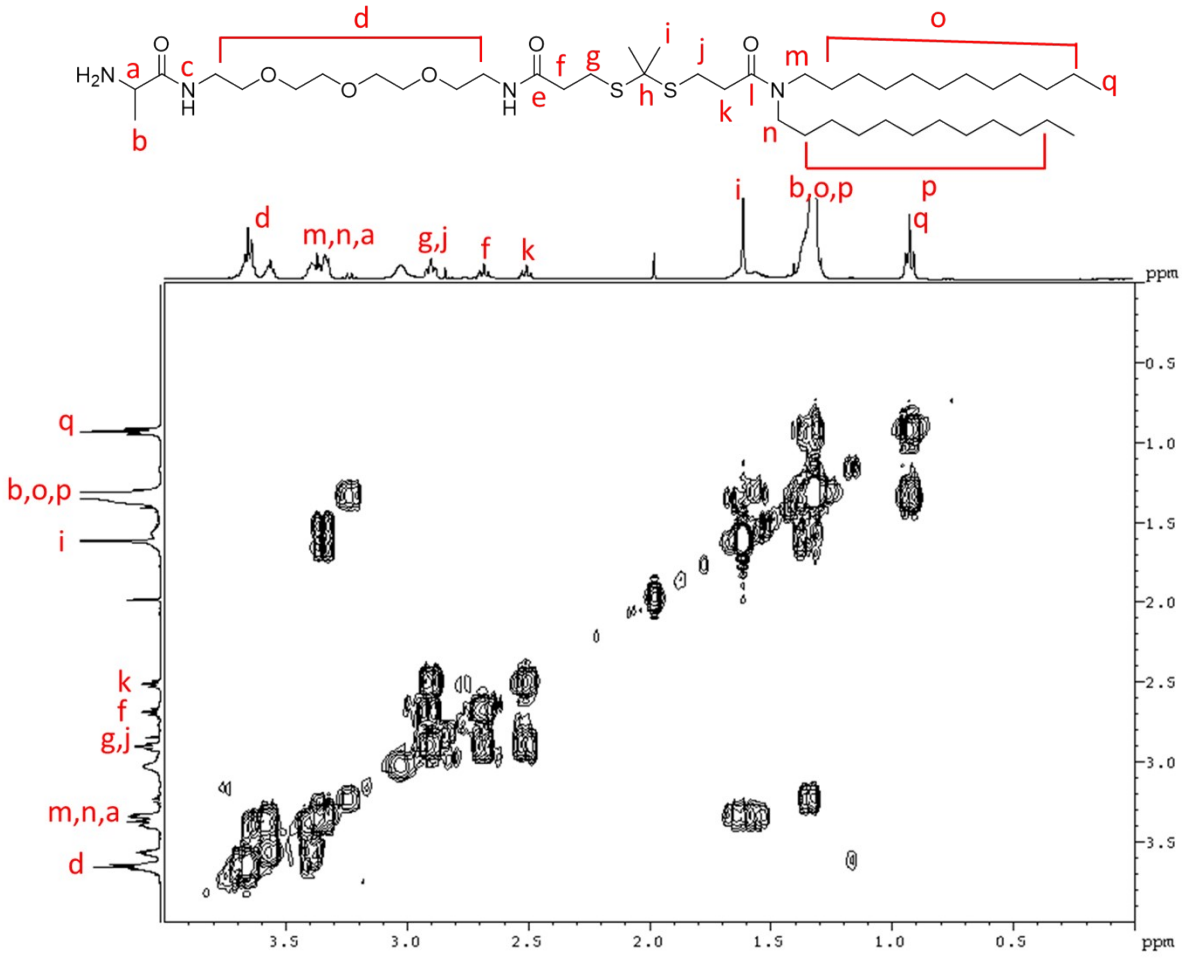

Fig S18. COSY NMR spectrum of Compound E.

24. Mass spectrum of Compound E

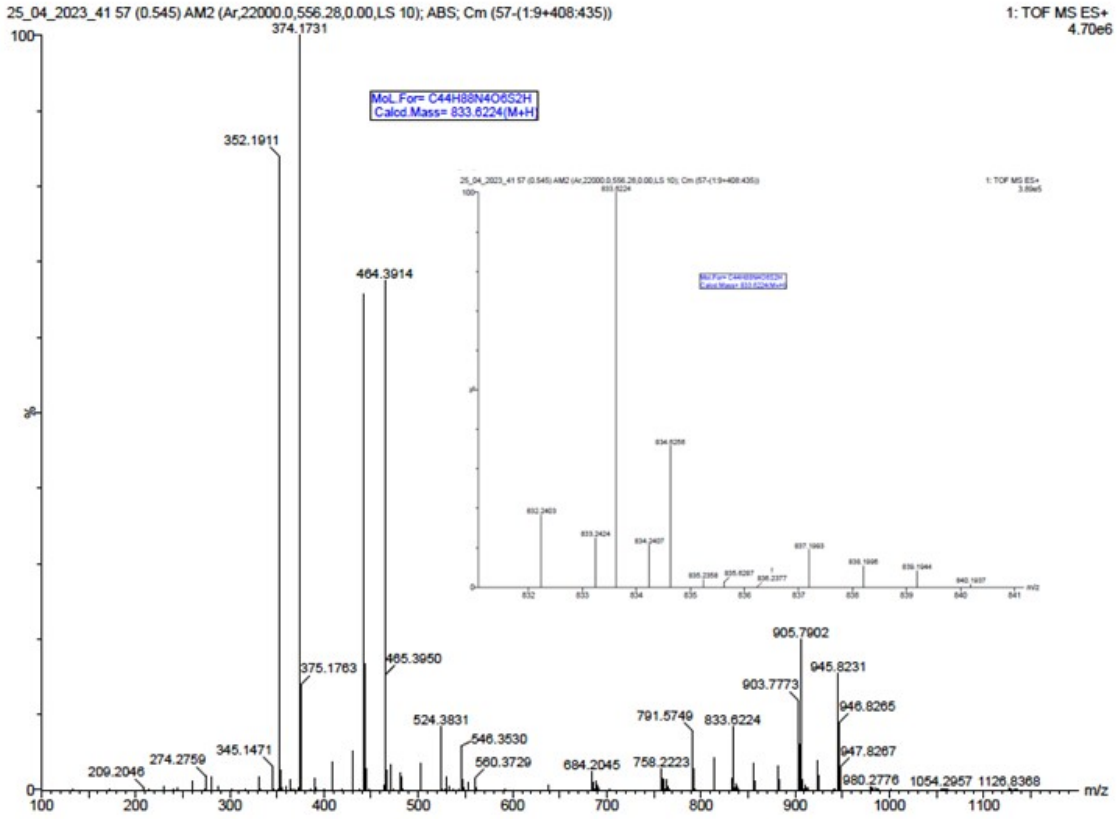

Fig. S19. Mass spectrum of Compound E. Inset: magnified view of the molecular ion region.

25. Characterization of SQDs

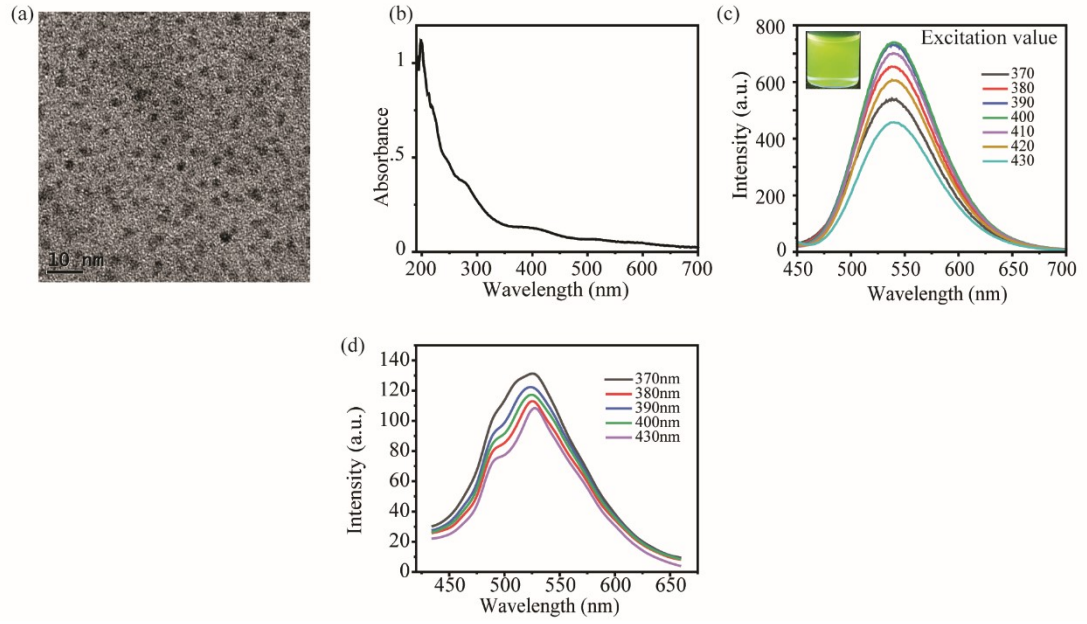

Fig. S20. (a) TEM image of SQDs. (b) UV-Vis spectra of SQDs in water. (c) Fluorescence emission spectra of SQDs in water. (d) Fluorescence emission spectra of SQD-loaded liposomes in water.

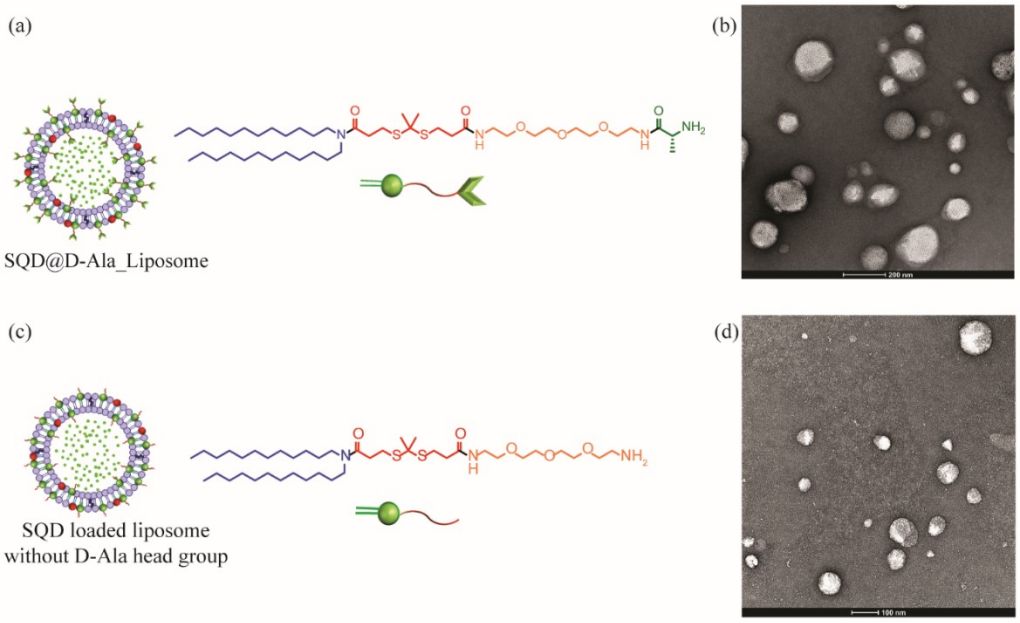

26. SQD loaded liposome with and without D-Ala head group

Fig. S21. (a) Schematic illustration and (b) TEM image of SQD loaded liposome with D-Ala head group (scale bar 200 nm). (c) Schematic illustration and (d) TEM image of SQD loaded liposome without D-Ala head group (scale bar 100 nm)

27. ^{1}H NMR spectra of positive thiol ligand

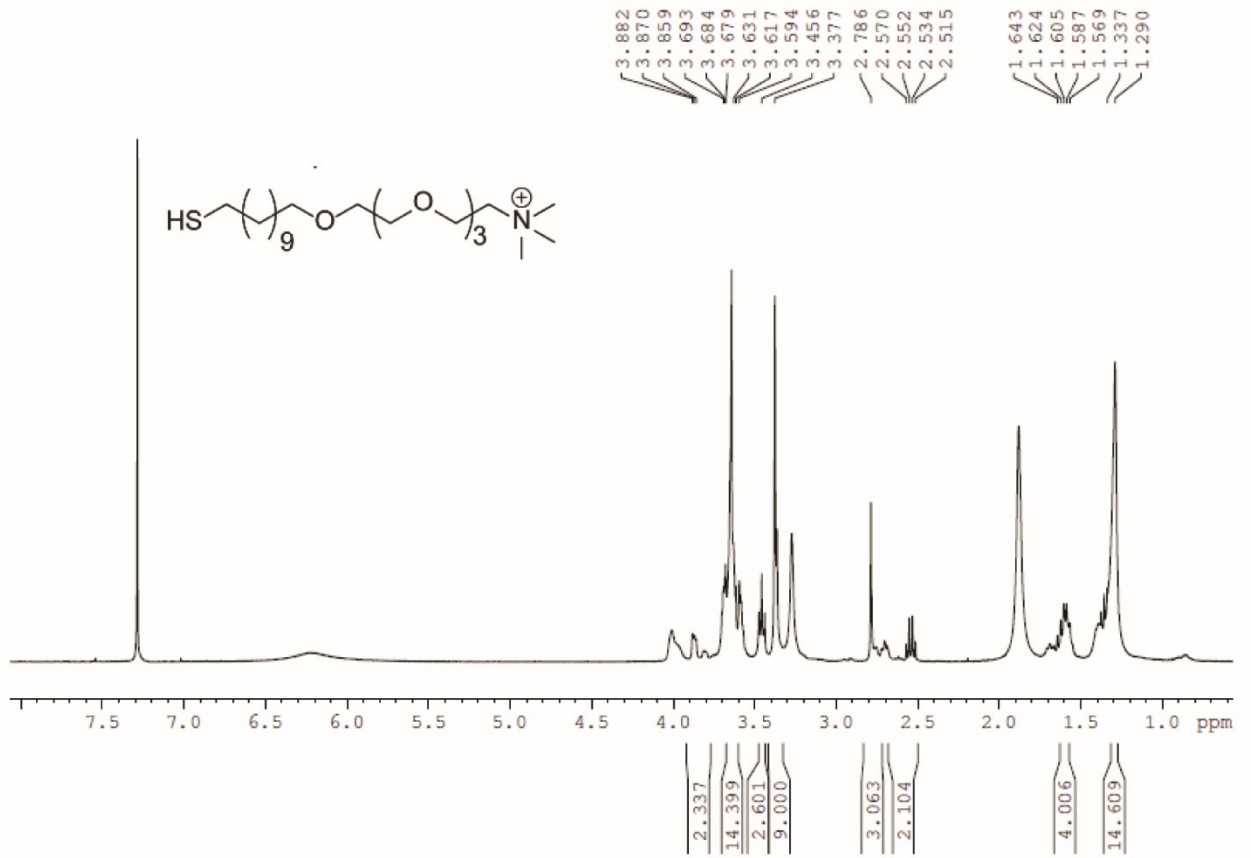

Fig. S22. ^{1}H NMR spectra of positive thiol ligand.

^{1}H-NMR (400 MHz, $CDCl_3$): δ 3.88-3.85 (bs, 2H, -CH_2-N+-), 3.69-3.67 (14H, -O-CH_2-CH_2-O-), 3.63-3.59 (t, 2H, -CH_2-**CH_2**-O-), 3.37 (s, 9H, -N+ $(CH_3)_3$), 2.78 (s, 3H, CH_3-SO_3-), 2.57- 2.51 (m, 2H, -CH_2-SH), 1.64-1.56 (m, 4H, -CH_2-), 1.33-1.29 (m, 14H, -CH_2).

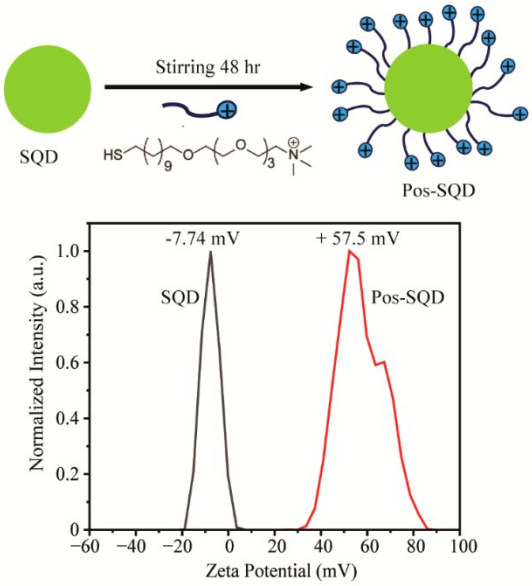

28. Functionalization of SQD by positive thiol ligand

Fig. S23. Functionalization of SQD by positive thiol ligand. The shift in zeta potential confirms the effective surface functionalization.

29. Antibacterial activity of only liposome

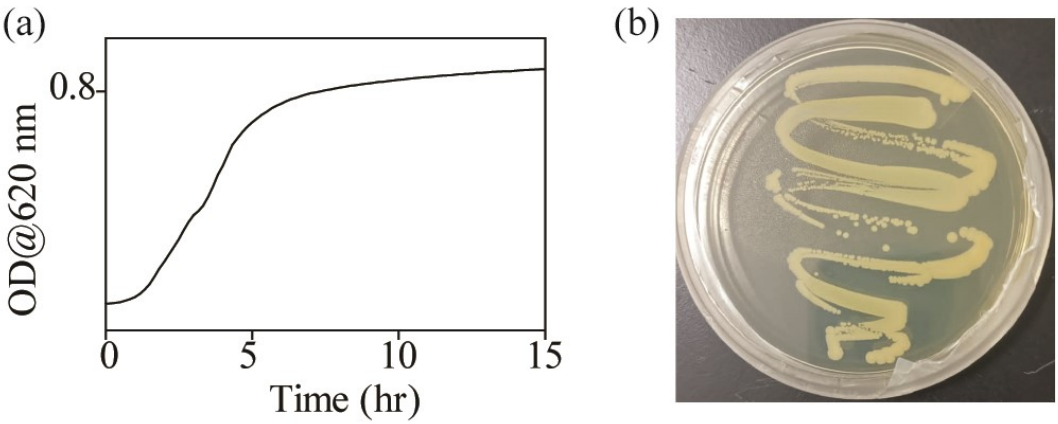

Fig S24. (a) Growth kinetics of MRSA bacteria in the dark in the presence of neat liposomes. (b) Growth of MRSA bacteria after 2 hours of incubation in the dark followed by 1 hour of light irradiation. Concentration of liposome: 0.65 μM of synthesized lipid.

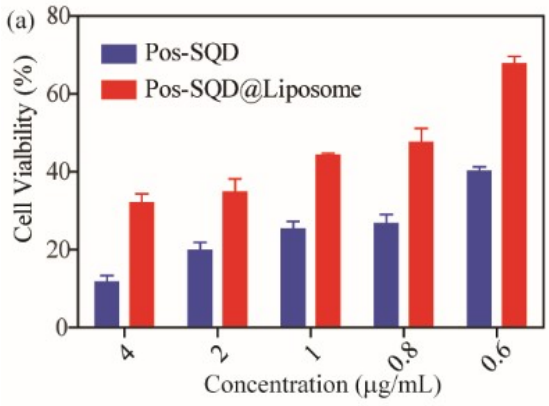

30. Cellular Viability

Fig. S25. (a) Viability of *HeLa* cells against Pos-SQD and Pos-SQD@Liposome.

References

1. R. L. Ball, P. Bajaj and K. A. Whitehead, *Int J Nanomedicine*, 2017, **12**, 305-315.
2. K. A. Whitehead, J. R. Dorkin, A. J. Vegas, P. H. Chang, O. Veiseh, J. Matthews, O. S. Fenton, Y. Zhang, K. T. Olejnik, V. Yesilyurt, D. Chen, S. Barros, B. Klebanov, T. Novobrantseva, R. Langer and D. G. Anderson, *Nat. Commun.*, 2014, **5**, 4277.
3. A. Mondal, S. Pandit, J. Sahoo, Y. Subramaniam and M. De, *Nanoscale*, 2023, **15**, 18624-18638.